Electrochimica Acta 55 (2010) 1013–1018

Contents lists available at ScienceDirect

Electrochimica Acta

journal homepage: www.elsevier.com/locate/electacta

Electrochemical intercalation of potassium into graphite in KF melt

Dongren Liu[a,c], Zhanhong Yang[a,*], Wangxing Li[b], Shilin Qiu[b], Yingtao Luo[b]

[a] College of Chemistry and Chemical Engineering, Central South University, South Lushan Road, Changsha 410083, Hunan, PR China
[b] Zhengzhou Research Institute of Chalco, Zhengzhou 450041, Henan, PR China
[c] Department of Chemical and Environmental engineering, Jiaozuo University, JiaoZuo 454003, Henan, PR China

ARTICLE INFO

Article history:
Received 6 August 2009
Received in revised form
22 September 2009
Accepted 25 September 2009
Available online 4 October 2009

Keywords:
Electrochemical intercalation
Potassium
Graphite
Molten potassium fluoride
Aluminum electrolysis

ABSTRACT

Electrochemical intercalation of potassium into graphite in molten potassium fluoride at 1163 K was investigated by means of cyclic voltammetry, galvanostatic electrolysis and open-circuit potential measurements. It was found that potassium intercalated into graphite solely between graphite layers. In addition, the intercalation compound formed in graphite bulk in molten KF was quite unstable and decomposed very fast. X-ray diffraction measurements indicate that a very dilute potassium–graphite intercalation compound was formed in graphite matrix in the fluoride melt. Analysis with scanning electron microscope and transmission electron microscope shows that graphite was exfoliated to sheets and tubes due to lattice expansion caused by intercalation of potassium in molten KF.

1. Introduction

Aluminum is conventionally manufactured by Hall-Héroult electrolysis process at high temperature (around 1233 K). Carbon anodes are consumed and carbon dioxide is emitted during the process. It is a challenge for the aluminum industry worldwide to replace the carbon anode with inert anode so as to avoid consumption of carbonous materials, and most importantly, to eliminate the emission of greenhouse gas. Research on inert anodes for aluminum electrolysis has been carried out for several decades. However, only limited progress has been made in this field because the inert anodes are severely eroded by the high-temperature melts in the conventional Hall-Héroult process [1,2]. Low temperature electrolytes, especially those with a melting point below 1023 K, could increase the probability of finding a suitable inert anode material because the corrosion rate of inert anode would greatly be reduced at low temperature [3–5].

As compared with the $NaF–AlF_3$ system, the $KF–AlF_3$ system seems to be a promising candidate as low temperature electrolyte due to its lower eutectic temperature and higher alumina solubility. The eutectic temperature of $KF–AlF_3$ system is around 833 K while that of $NaF–AlF_3$ system is around 971 K [6]. The studies on $KF–AlF_3$-based electrolyte system were mainly focused on its physical or chemical properties and corrosion effects on inert anodes [6–9]. Penetration of the electrolyte into the cathode carbon block, however, is important since it affects the cell life in aluminum reduction cell. Although the inert cathode materials (wettable cathode) in which TiB_2 is the main component in either pure form or composite could be applied to a carbon lining, which may help to reduce the melt penetration and prolong cathode lifetime in the industrial cell [10], better understanding of potassium interaction with cathodic carbon block would be of basic importance to predict the performance of cathode when $KF–AlF_3$ system is used as low temperature electrolyte.

It has been found that potassium could intercalate into graphite lattice to form potassium–graphite intercalation compounds (K-GICs) with various stage structure either at relatively low temperature or in organic solutions [11–14]. However, it may not be the case for intercalation occurring between potassium and carbon in molten fluoride salt. Electrochemical intercalation of alkaline metals such as lithium and sodium into graphite in molten chloride has been employed to produce nano-sized carbon materials like tubes and particles [15–18]. Also, the intercalation of potassium into graphite by electrolysis in chloride melt has been reported and investigated for the mechanism in order to elucidate the role of potassium intercalation in the formation process of nano-sized carbon materials [19,20]. In the present work, the basic mechanism of potassium intercalation into graphite in the pure KF melt under cathodic polarization condition was discussed, with the aim of understanding the electrochemical intercalation process of potassium and the nature of the intercalation resultants.

* Corresponding author. Tel.: +86 731 8836618; fax: +86 731 8879616.
E-mail address: zhyang@mail.csu.edu.cn (Z. Yang).

0013-4686/$ – see front matter © 2009 Elsevier Ltd. All rights reserved.
doi:10.1016/j.electacta.2009.09.072

2. Experimental

Anhydrous potassium fluoride contained in a graphite crucible was heated up to 523 K and held at this temperature for 8 h under vacuum, then heated up to the working temperature 1163 K, which is higher than the melting point of KF (1131 K). Electrochemical experiments were performed with a three-terminal electrochemical cell. The graphite crucible served as the container for the electrolyte and also as the high surface counter electrode. The working electrode (WE) was a thin sheet (with a dimension of 5.9 mm wide × 4 mm high × 1.2 mm thick exposed to molten salt) machined from a spectral pure graphite rod (d_{002} = 0.337 nm, crystallite size along *c*-axis L_c = 69 nm, apparent density = 1.78 g cm^{-2}, open porosity = 20.9%). The rest of graphite rod was shielded with BN tube. A stainless steel rod was connected to the graphite rod as current lead. Due to the difficulty of finding a suitable reference electrode in molten KF, platinum wire of 1.0 mm diameter was employed as the quasi-reference electrode. Hence, all potentials in the present work are expressed versus the platinum reference electrode. The stability of the quasi-reference electrode was confirmed by measuring the potential difference between two platinum wires in molten potassium fluoride for 12 h. It was found that the potential fluctuation of Pt electrode did not exceed ±10 mV. The graphite crucible was placed inside a sintered corundum tube within a programmable vertical furnace. The electrochemical cell was under a continuous nitrogen circulation during the experiment. Electrochemical measurements were performed with a PAR Model 263A Potentiostat/Galvanostat monitored by a computer with commercial PowerSuit software.

At first, the WE was characterized by means of cyclic voltammetry. Around 70% of the measured solution resistance between the working and reference electrodes was compensated for all cyclic voltammetric measurements. Secondly, the WE was subjected to galvanostatic electrolysis. Once the current was shut down, the open-circuit potential (OCP) of the WE was traced. After OCP measurements, the electrode was removed from the melt and cooled down naturally in nitrogen atmosphere. The electrode was washed with distilled water to get rid of the solidified electrolyte on the electrode surface. Scanning electron microscope (SEM) performed on JSM-6360LV (JEOM) was utilized to investigate the surface morphology of the electrode. In another case, the electrode just undergone galvanostatic electrolysis was taken out of the melt immediately, then cooled down rapidly in nitrogen atmosphere to room temperature and transferred into a glove box filled with high purity nitrogen. The graphite sheet was ground to powder and sealed with polyethylene film for X-ray diffraction (XRD) measurements which were performed on X′Pert Pro diffractometer (PANalytical) with Cu Kα radiation. Finally, after conducting galvanostatic electrolysis, a thin upper layer of solidified electrolyte in the cooled down graphite crucible was sampled to a 50-ml beaker. Then 30 ml of distilled water was added to the beaker and sonicated for 10 min. The aqueous mixture was left to stand overnight. Samples collected from the surface of the aqueous mixture by a pipette were dripped onto a holey carbon coated copper grid and then dried thoroughly for transmission electron microscope (TEM) analysis which was performed on JEM-2100 (JEOM, 200 keV, capable of energy dispersive X-ray analysis).

3. Results and discussion

3.1. Cyclic voltammetry

Potassium is soluble in molten potassium fluoride [21]. Furthermore, as reported in ref. [20], considerable evaporation of potassium occurred in the process of cathodic polarization as the working temperature (1163 K) is higher than the boiling point of potassium (1032 K). The interference of these two factors with potassium intercalation into graphite may influence the magnitude of the current that is attributed solely to the latter process. In order to evaluate the disturbance amplitude of potassium dissolution and evaporation, cyclic voltammogram was recorded on platinum electrode in molten KF at a scan rate of 100 mV s^{-1} at 1163 K (Fig. 1). Platinum electrode was chosen to estimate the current density caused by potassium dissolution and evaporation due to its chemical inertness against potassium and fluoride melt. The voltammogram in Fig. 1 shows potassium deposits at the potential of ca. −1.1 V. It is notable that the oxidation peak of potassium is absent during the anodic scan even when the cathodic potential is down to −1.5 V. That strongly indicates that potassium deposited in cathodic process undergoes very rapid dissolution and evaporation. That is, metallic potassium generated at the cathodic sweep had completely escaped from the electrode surface before the sweep was reversed to its oxidation potential at the potential scan rate, which is in agreement with that reported by Chen et al. [20].

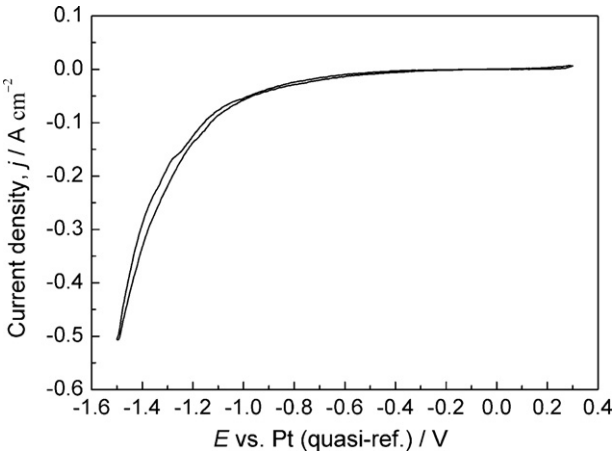

Fig. 1. Cyclic voltammogram recorded on platinum electrode in molten KF at 1163 K. Potential scan rate = 100 mV s^{-1}.

Fig. 2 presents cyclic voltammograms recorded on the platinum wire and the graphite sheet electrode in molten potassium fluoride at 1163 K. The potential was scanned from a potential at which no reduction or oxidation reaction occurred in the negative direction and switched at −1.1 V to avoid the deposition of metallic potassium at a scan rate of 100 mV s^{-1}. The cyclic voltammetric behavior of graphite differs greatly from that of platinum. A reduction wave starts from around −0.8 V on graphite electrode, and then the cur-

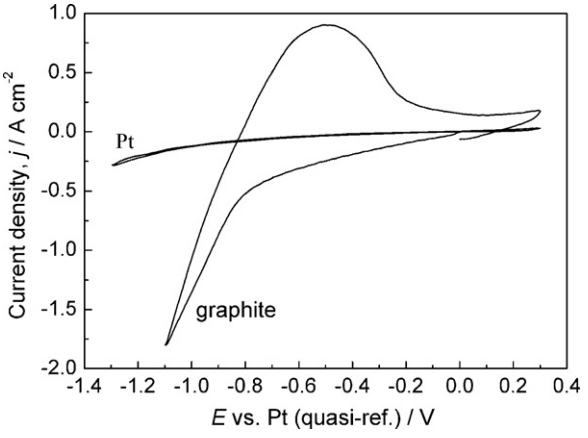

Fig. 2. Cyclic voltammograms recorded on graphite and platinum electrode in molten KF at 1163 K. Potential scan rate = 100 mV s^{-1}.

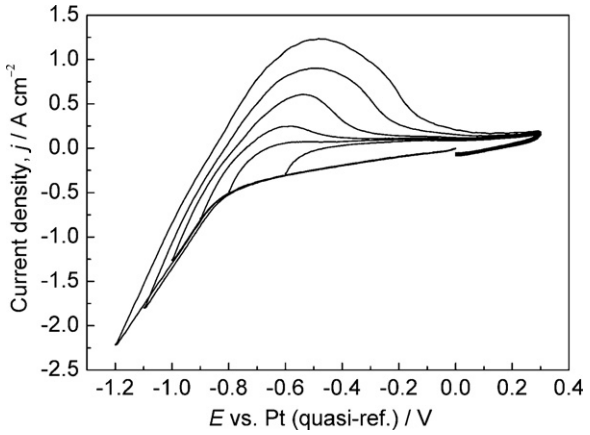

Fig. 3. A series of cyclic voltammograms recorded on graphite electrode with various cathodic switch potential in molten KF at 1163 K. Potential scan rate = 100 mV s^{-1}.

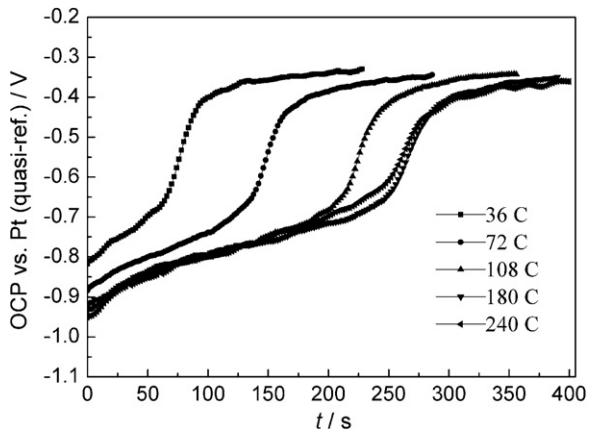

Fig. 4. OCP variations of the graphite electrodes after galvanostatic electrolysis in molten KF at 1163 K. The inserted numbers behind the legends denote the transferred electricity during galvanostatic electrolysis.

rent density increases with accelerated speed. An anodic wave is found in the reverse potential scan. It is the same as on platinum electrode, no anodic wave would be found if the cathodic wave is supposed to deposition of metallic potassium on graphite electrode. It is because of the fact that the metal would have escaped from the surface of electrode completely before the sweep is reversed to its oxidation potential due to severe dissolution and evaporation. On the other hand, the cathodic current density recorded on the graphite electrode is much larger than that on platinum. So it is reasonable to ascribe the coupled cathodic and anodic waves recorded on graphite electrode to potassium intercalation into and extraction from graphite lattice respectively instead of deposition and stripping of metallic potassium. It is easy to find that potassium ion discharges at a slightly more positive potential on graphite than on platinum. The reason for that potential shift is due to the intercalation of potassium into the graphite bulk. It is worthy of noting that the anodic current density is much lower than cathodic current density, indicating that the K-GIC (potassium–graphite intercalation compound) produced at cathodic scan probably undergoes decomposition or kinetic limitations are involved in the anodic reaction instead of dissolution and evaporation of metallic potassium. Fig. 2 also shows an unsymmetrical shape with extra broad width for the anodic wave of the cyclic voltammogram on graphite electrode. The shape of anodic wave indicates that kinetic limitations such as charge transfer or phase transition are probably involved in the process of anodic reaction. It should be also noted that relatively higher reduction current density is observed on graphite electrode as compared with that on the Pt electrode in the potential range from the onset of sweep to −0.8 V in the cathodic direction. It is probably due to the intercalation of potassium into the graphite lattice. In order to confirm whether the intercalation reaction is involved in this potential range or not, more cyclic voltammetric experiments with various negative switch potentials were carried out.

Fig. 3 shows a series of cyclic voltammograms on graphite electrode with different cathodic switch potentials. When the sweep is reversed at potential more positive than −0.8 V, no anodic wave is observed in the reverse sweep, suggesting that no intercalation reaction occurs when the potential is more positive than −0.8 V. The current is probably caused by the electro-endosmosis of electrolyte into the interior of graphite electrode, which is confirmed by the subsequent XRD measurements in this paper. When the sweep is reversed at more negative switch potential, no other cathodic or anodic waves are observed except the current density of cathodic and anodic wave increase monotonically, suggesting that only potassium intercalation is involved in the cathodic process. It is quite different from the process of sodium intercalation into graphite in cryolite melts which is always accompanied by the insertion of metallic sodium to the micropores of the graphite bulk [22,23].

3.2. OCP variation of K-GIC

Fig. 4 presents the OCP variations of intercalated graphite after galvanostatic electrolysis with various amounts of transferred charges at a current magnitude of 200 mA. All the curves show similar shape. The curves start from various onsets of open-circuit potential which gets more negative as the amount of transferred charge increases. Then the curves ascend gradually and rise abruptly at the open-circuit potential of ca. −0.65 V, which can be assigned to the decomposition and disappearance of K-GIC. It is worthy of noting all the curves present slowly ascending slope rather than plateau within the potential range from the onset to −0.65 V, which is probably because of the variation of K-GIC concentration in graphite matrix. The length of the slope representing the lifetime of the K-GIC is relatively short. It implies K-GIC is quite unstable in molten KF and suffers from fast decomposition, in agreement with the cyclic voltammetric results. The OCP curves become nearly overlapped with each other as the transferred charge increases, which means that potassium reaches the maximum concentration in graphite and probably the metallic potassium starts to deposit on electrode under the current conditions. The deposition of metallic potassium is confirmed by the chronopotentiometric experiment as presented in Fig. 5. It can be seen from the chronopotentiogram that the potential decreases gradually versus time. It is because of the fact that the rising potassium concentration in the graphite bulk requires an increasingly larger voltage to maintain a constant current through the electrode. The potential of working electrode gets to −1.1 V when the transferred charge reaches 180 C, a potential at which deposition of metallic potassium occurs.

Phase transition is a general phenomenon in the process of forming graphite intercalation compounds. A typical example is the lithium intercalation into graphite in Li-ion battery which comprises a series of stage transformations between distinct stages [24,25]. These phase transformations can be identified by distinct potential plateaus on the charge curve or coulometric titration curve. From the distinct onset of OCP curves, one would infer that stage transformation may be probably involved in the process of potassium intercalation. As for the intercalation of potassium into graphite in molten KF, it is difficult to perform small rate intercalation or coulometric titration due to the fast decomposition of

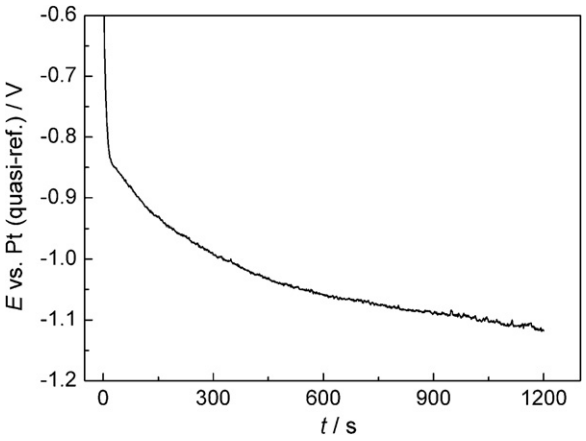

Fig. 5. Chronopotentiogram of graphite electrode in molten KF during cathodic polarization with at 1163 K. Step current = 200 mA.

K-GIC. So XRD measurements were carried out in order to check the occurrence and stage structure of K-GIC formed by electrolysis.

3.3. XRD characterization of the electrolysis resultants

The graphite was subjected to galvanostatic electrolysis until 72 C, 108 C and 180 C electricity was transferred for XRD measurements, respectively. Fig. 6 presents the XRD patterns of the resultant compounds after electrolysis as well as pristine graphite. The diffraction lines at 29°, 33.6°, 48.2°, 57.2°, 60° and 70.5° can readily be identified as KF crystal. Matched with the cyclic voltammetric result, it is supposed that the KF results from electro-endosmosis of molten salt into micropores of graphite bulk under cathodic polarization condition. The lines at 21.5°, 23.9° and 36.3° in 2θ are assigned to polyethylene. Also, the diffraction line of pristine host can be found at 26.5°. Only the weak line at 27.3° in 2θ, which is partly overlapped with the line 0 0 2 of pristine graphite, is related to K-GIC. There is however no evidence for the occurrence of potassium carbide in the XRD patterns despite the high working temperature. The *c*-axis repeat distance of K-GIC, I_c, can be determined from this peak using Eq. (1)

$$I_c = l \times d_{00l} \tag{1}$$

where l is an integer and d_{00l} can be calculated from Bragg equation. Then the stage number of K-GIC is determined from I_c using

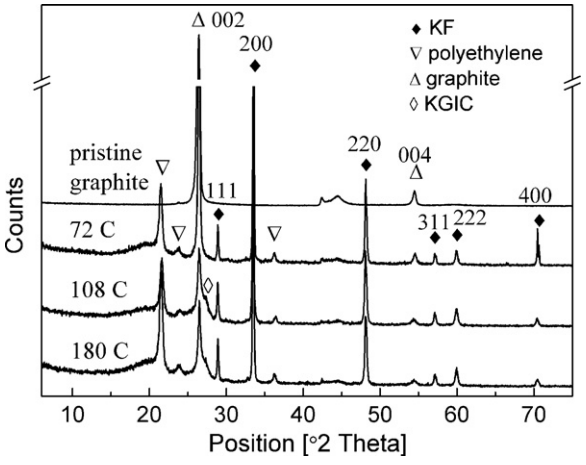

Fig. 6. X-ray diffraction patterns of resultant compounds after galvanostatic electrolysis in molten KF at 1163 K.

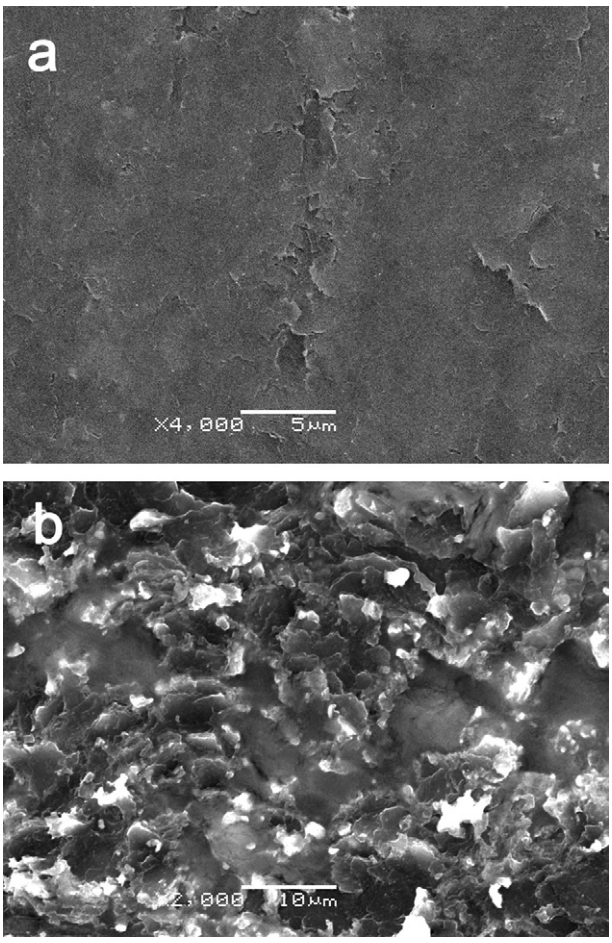

Fig. 7. SEM photographs of graphite electrodes surface: (a) before electrolysis; (b) after electrolysis—note that the electrode was washed with distilled water to get rid of the solidified electrolyte on surface.

the Eq. (2).

$$I_c = nc_0 + d_i = (n-1)c_0 + d_s \tag{2}$$

where n is the stage number, c_0 is the interplanar distance of the pristine graphite layers ($c_0 = 0.337$ nm) and $d_s = c_0 + d_i$ is the distance separating two graphite layers between which an intercalate layer is sandwiched ($d_s = 0.541$ nm for K-GIC) [26]. The *c*-axis repeat distance is determined as $I_c = 3.912$ nm, which is very close to the calculated I_c value of 3.911 nm for stage-11 K-GIC according to Eq. (2). The determined I_c value indicates that a higher stage K-GIC was formed by electrolysis in the fluoride melt. However, the stage number of K-GIC could not be accurately evaluated because only one diffraction line related to it was observed. It is noticed that the peak at 27.3° is absent in the sample which was subjected to electrolysis with 72 C electricity. That is probably due to the complete decomposition of K-GIC during the cooling process. The XRD patterns of K-GICs show almost identical characteristics despite being formed by electrolysis with different electricity. Coupled with the behavior of OCP variations, it can be inferred that only higher stage K-GIC was generated in molten KF. Consequently, no stage transformation occurred in the process of potassium intercalation and extraction.

3.4. SEM and TEM characterization

The surface morphology images of graphite electrode before and after electrolysis are depicted in Fig. 7. The electrode before electrolysis owns a scale-like surface (Fig. 7a). After electrolysis, the

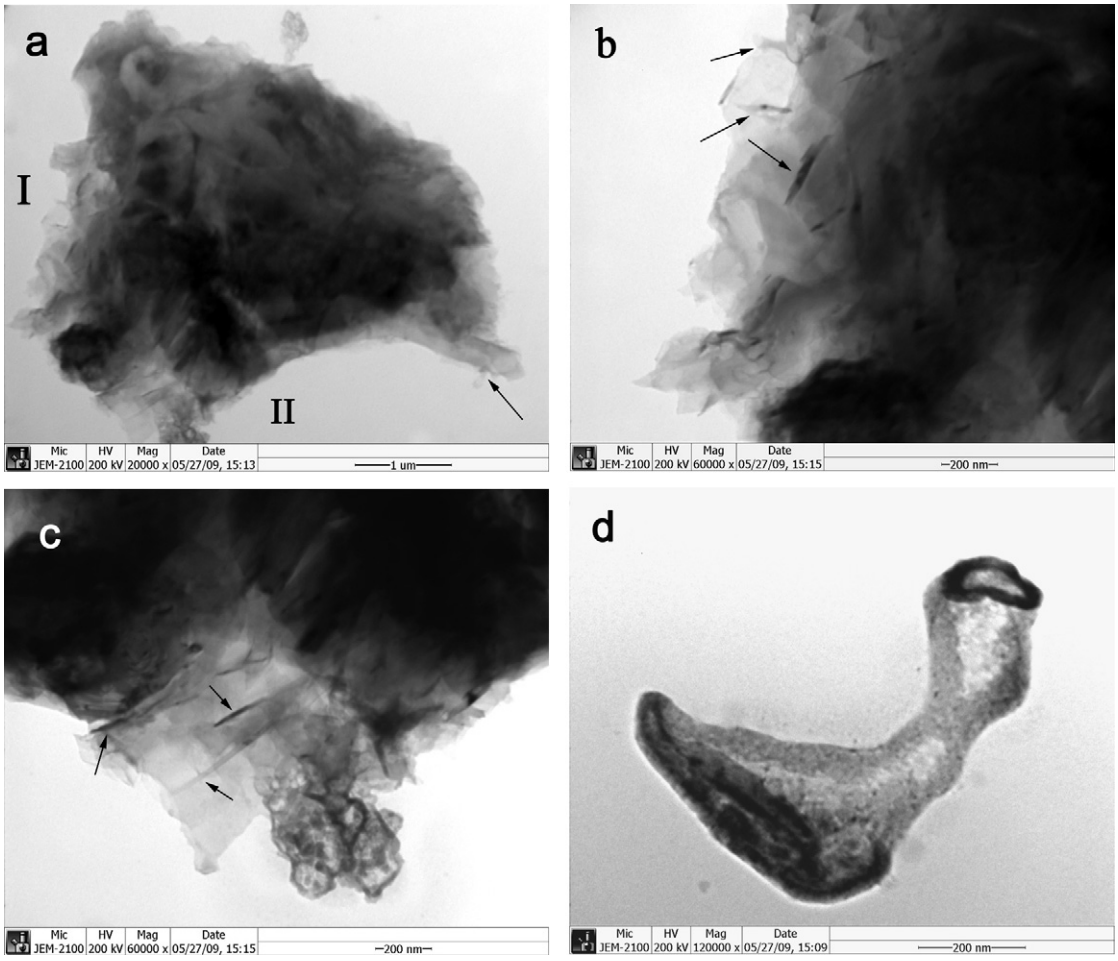

Fig. 8. TEM images of: (a) a representative sample obtained at the upper layer of the melts; (b) magnified image of local region I marked in photograph (a); (c) magnified image of local region II marked in photograph (a); (d) an individual dumbbell-like tube. The arrow marked in image (a) points to a tube. The arrows marked in image (b) and (c) point to the enrolled edges of thin sheets.

electrode is severely eroded as many irregular crystal facets and concaves can readily be observed (Fig. 7b). Similar behavior was observed during electrolysis in molten alkali chloride using carbon as cathode [16]. It is believed that the crystal facets and concaves are caused by the exfoliation of graphite layers and particles. As proposed by Chen et al. [20], in the process of potassium intercalation, potassium atoms entered into the interlayer of graphite and led to strong lattice expansion due to the large ionic radius of potassium whereafter resulted in some of graphite layers and particles stripping from the graphite bulk. The stripping process was facilitated by the weakened interaction between adjacent graphite layers under high temperature. Only the electrode suffered from electrolysis with 108 C transferred charges was examined with SEM analysis because those electrodes with large charge transferring were cracked to fragments when they were washed with distilled water due to seriously destroyed texture of the graphite caused by the lattice expansion.

TEM together with energy dispersive X-ray analysis (EDX) has been employed to identify the nature of the exfoliations from electrode. Generally, the exfoliations were found to be aggregated in various dimensions. Fig. 8a shows the TEM image of a representative example of the exfoliations floated in the surface of fused KF. From the edge of aggregate presented in Fig. 8a, extremely thin sheets can be seen. Fig. 8b and c gives magnified images of the local regions I and II marked in Fig. 8a respectively for closer observation of the thin sheets. The individual sheet can be well discerned from the huddle by the enrolled edge (marked in Fig. 8b and c with arrows). Also, some sheets have totally enrolled to form tubes in a state of single (Fig. 8d) or aggregate (marked in Fig. 8a with an arrow). The components of sheet and tube were confirmed to be carbon by EDX analysis (Fig. 9). The thickness of the sheets varies from ca. 10 nm to 20 nm, much less than the crystallite size along *c*-

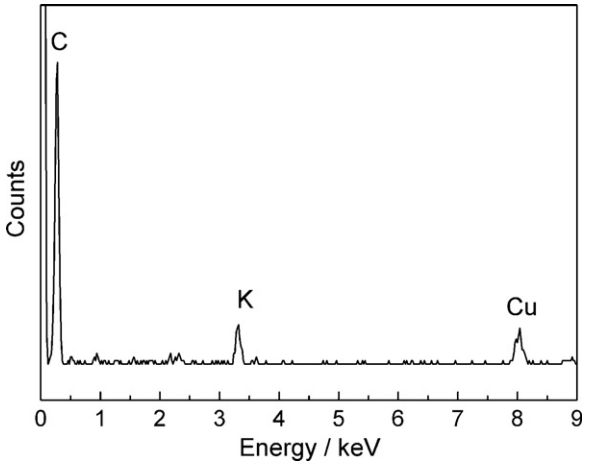

Fig. 9. Typical EDX spectrum of the sample shown in Fig. 8. The Cu and K profiles were built up from a TEM copper grid and the not completely removed electrolyte respectively.

axis (69 nm) of the pristine graphite used in experiments. Coupled with the SEM analyses, evidently the sheets are fragments stripped from the graphite crystal by potassium intercalation. However, neither single wall nor multiple wall nanotubes were observed in the samples, which is different from the reported results that examples of nanotubes were found after intercalation of potassium into graphite in molten chloride [19,20].

4. Conclusions

It was found that potassium intercalated into graphite electrode in the cathodic polarization process in molten potassium fluoride. The intercalation proceeded solely via the mechanism of intercalation between graphene layers. Higher stage potassium–graphite intercalation compound was detected in graphite electrode after galvanostatic electrolysis by X-ray diffraction analyses. Moreover, the intercalation compound was quite unstable and decomposed very fast under the experimental conditions in the present work. SEM analyses show the graphite electrode was severely eroded after galvanostatic electrolysis due to exfoliation of graphite layers and particles. TEM coupled with EDX examinations indicates that the exfoliations resulted from the potassium intercalation were aggregate of thin graphite sheets or tubes. The SEM and TEM results offer clear evidences that intercalation of potassium into graphite occurred indeed. These findings could provide a deeper understanding of the basic mechanism of potassium interaction with cathodic carbon block in the Hall-Héroult process when potassium cryolite would be used as low temperature electrolyte.

Acknowledgements

The finance supported by Hunan Province innovation foundation for postgraduate is acknowledged. The authors wish to thank the referees and editors for their valuable suggestions and assistances in improving this paper.

References

[1] J.K. Walker Kinkoph, C.K. Saha, J. Appl. Electrochem. 19 (1989) 225.
[2] J.A. Sekhar, J. Liu, H. Deng, J.J. Duruz, V. de Nora, Light Metals (1998) 597.
[3] J. Thonstad, E. Olsen, JOM 53 (2001) 36.
[4] V. Blinov, P. Polyakov, J. Thonstad, V. Ivanov, E. Pankov, Aluminum 73 (1997) 906.
[5] V. Blinov, P. Polyakov, J. Thonstad, V. Ivanov, E. Pankov, Aluminium 74 (1998) 349.
[6] E. Robert, J.E. Olsen, V. Danek, E. Tixhon, T. Østvold, B. Gilbert, J. Phys. Chem. B 101 (1997) 9447.
[7] J. Híveš, J. Thonstad, Electrochim. Acta 49 (2004) 5111.
[8] J. Yang, J.N. Hrynl, B.R. Davis, Alain Roy, G.K. Krumdick, J.A. Pomykala, Light Metals (2004) 321.
[9] Y. Zaikov, A. Khramov, V. Kovrov, V. Kryukovsky, A. Apisarov, O. Tkacheva, O. Chemesov, N. Shurov, Light Metals (2008) 505.
[10] J. Thonstad, P. Fellner, G.M. Haarberg, J. Híveš, H. Kvande, Â. Sterten, Aluminium Electrolysis: Fundamentals of the Hall-Hérout Process, third edition, Aluminium-Verlag, Dusseldorf, Germany, 2001, p. 333.
[11] W. Oh, S. Cho, Y. Ko, Carbon 34 (1996) 209.
[12] S. Aronson, F.J. Salzano, D. Bellafiore, J. chem. Phys. 49 (1986) 434.
[13] Y. Mizutani, T. Abe, K. Ikbda, E. Ihara, M. Asano, T. Harada, M. Inana, Z. Ogumi, Carbon 35 (1997) 61.
[14] Y. Mizutani, T. Abe, M. Inaba, Z. Ogumi, Synth. Metals 125 (2002) 153.
[15] W.K. Hsu, J.P. Hare, M. Terrones, H.W. Kroto, D.R.M. Walton, P.J.F. Harris, Nature 377 (1995) 687.
[16] W.K. Hsu, M. Terrones, J.P. Hare, H. Terrones, H.W. Kroto, D.R.M. Walton, Chem. Phys. Lett. 262 (1996) 161.
[17] Q. Xu, C. Schwandt, G.Z. Chen, D.J. Fray, J. Electroanal. Chem. 530 (2002) 16.
[18] A.T. Dimitrov, G.Z. Chen, I.A. Kinloch, D.J. Fray, Electrochim. Acta 48 (2002) 91.
[19] G.Z. Chen, X. Fan, A. Luget, M.S.P. Shaffer, D.J. Fray, A.H. Windle, J. Electroanal. Chem. 446 (1998) 1.
[20] G.Z. Chen, I. Kinloch, M.S.P. Shaffer, D.J. Fray, A.H. Windle, High Temp. Mater. Processes 2 (1998) 459.
[21] J.W. Johnson, M.A. Bredig, J. Phys. Chem. 62 (1958) 604.
[22] N. Adhoum, J. Bouteillon, D. Dumas, J.C. Poignet, Electrochim. Acta 51 (2006) 5402.
[23] P.Y. Brisson, H. Darmstadt, M. Fafar, A. Adnot, G. Servant, G. Soucy, Carbon 44 (2006) 1438.
[24] J.R. Dahn, Phys. Rev. B 44 (1991) 9170.
[25] J.R. Dahn, R. Fong, M.J. Spoon, Phys. Rev. B 42 (1990) 6424.
[26] M.S. Dresselhaus, G. Dresselhaus, Adv. Phys. 51 (2002) 1.